

[6]

Microearthquake seismicity and active tectonics of northwestern Greece

G.C.P. King¹, A. Tselentis^{1,*}, J. Gomberg^{2,**}, P. Molnar², S.W. Roecker²,
H. Sinvhal³, C. Soufleris^{1,‡} and J.M. Stock^{2,‡‡}

¹ Bullard Laboratories, Department of Earth Sciences, Madingley Rise, Madingley Road, Cambridge, CB3 0EZ (England)

² Department of Earth and Planetary Sciences, Massachusetts Institute of Technology, Cambridge, MA 02139 (U.S.A.)

³ Department of Earth Sciences, The University of Roorkee, Roorkee, U.P. (India)

Received June 21, 1983

Revised version received September 20, 1983

We carried out a microearthquake survey lasting for six weeks in northwest Greece using 18 portable seismograph stations to examine a region in which normal and thrust faulting have been reported in close proximity to one another. With this array we located 148 events and determined fault plane solutions for eight events using only rays radiated upwards. The seismicity of the region is diffuse with events extending to depths of nearly 30 km, and there is a minimum in activity near a depth of 15 km. The fault plane solutions exhibit a wide spectrum of fault types and orientations and are not consistent with simple zones of shortening or extension. Neither tractions applied to the edges or bottom of the region nor deviatoric stresses that compensate for lateral variations in crustal thickness can account for the variety of fault plane solutions. We think that the complicated behavior is a manifestation of inhomogeneous deformation due, at least in part, to a pre-existing complicated juxtaposition of structures and formations.

1. Introduction

The existence of regions of crustal extension within broad zones of continental convergence is well established, but the causes of the extension are a subject of controversy. Part of the poor understanding derives from scanty information. Moreover, data from different regions suggest that different extensional environments may require different physical explanations. For instance, some graben systems, such as the Baikal Rift system in

Siberia or the Shansi Graben in northeast China, appear to be driven at least in part by the collision of India with Eurasia, and crudely reflect a wedging apart of Asia by India [1,2]. Elsewhere some extension is very likely due to the release of gravitational potential energy stored in elevated mountainous regions and their associated crustal roots (e.g. Tibet [3] or Peru [4]). Extension can be enhanced by the subduction of small oceanic basins and the consequent seaward migration of the subduction zone with respect to large, converging plates (e.g. the East Carpathian arc and the Pannonian basin [5] or the Aegean arc and basin according to Le Pichon and Angelier [6]). Finally, a fourth possibility is that drag on the base of the lithosphere by small-scale convection in the asthenosphere might cause extension [7]. These mechanisms are not mutually exclusive and need not operate independently, but it appears that no

Present addresses:

* Royal School of Mines, Imperial College of Science and Technology, Prince Consort Road, London, England.

** Institute of Geophysics and Planetary Physics, University of California at San Diego, La Jolla, CA 92038, U.S.A.

‡ Greek Army, Athens, Greece.

‡‡ U.S. Geological Survey, Menlo Park, CA 94025, U.S.A.

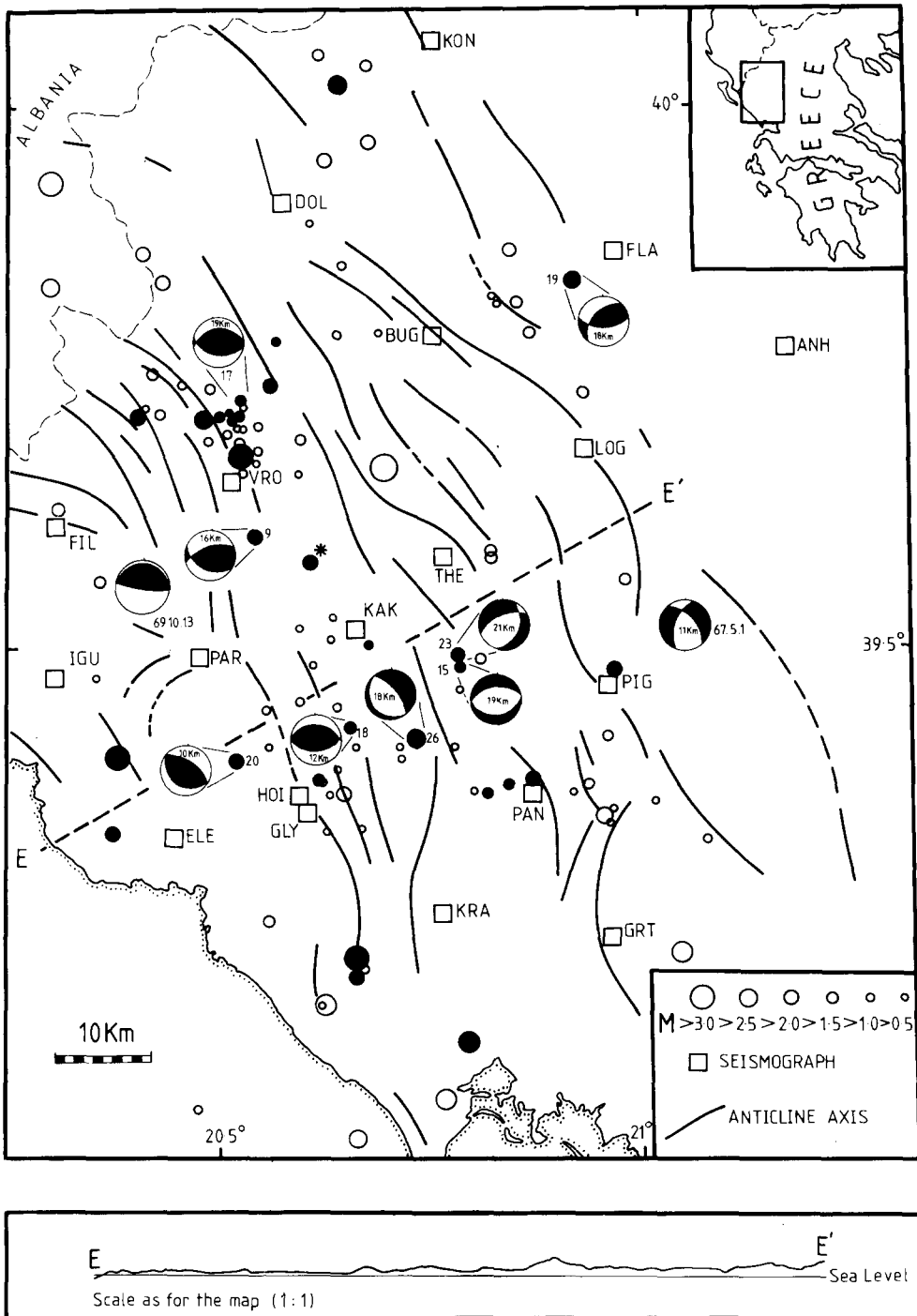


Fig. 1. Map showing the location of our 18 portable seismograph stations and the epicenters of 148 events located using this array (circles). Solid circles show the epicenters of the 30 best located events (see text). An asterisk shows the epicenter of an event with a depth of 29 km, and the depths of the events with fault plane solutions are written inside the balloons. The numbers that appear next to the events with fault plane solutions are the event reference numbers used in Fig. 4. The fault plane solutions of the events of 13 October 1969 [12] and 1 May 1967 [15] are plotted within the areas of maximum intensity and not at the epicenters calculated by the U.S. Geological Survey. The solid lines are axes of anticlines taken from reference 13. A topographic cross section, typical for the region, is shown below the map.

one mechanism is required for all extensional terrains within convergent zones. The results of the present study suggest further that local heterogeneities can perturb the regional, average, strain field by including both localized extension and shortening. These results re-emphasize the need for care in using localized observations to deduce regional strain (or stress) (e.g. [8]).

The Aegean region and its continuations into northern Greece, Albania and Yugoslavia and into western Turkey comprise an important zone of extension, if only because all of the mechanisms listed above have been applied to parts of this region (cf. [6,7,9,10]). Most of the Aegean has undergone crustal extension concurrently with subduction of the apparently oceanic lithosphere of the eastern Mediterranean beneath the Aegean arc (e.g. [6]). The mechanism of extension in western Turkey probably is related to the same process. At the same time, because extension and crustal thinning have not yet brought the region below sea level, a reduction of the horizontal compressive stresses possibly caused by a retreating trench system and the remaining, relatively large vertical stress where the crust is thick may be adequate to explain extension in western Turkey and possibly the Aegean region.

In northwest Greece, Albania and Yugoslavia, however, these conceptually simple mechanisms seem to be inadequate to account for the extension. West of northern Greece and Albania there appears to be no oceanic lithosphere; instead thicker, probably thin continental, crust beneath the Adriatic Sea may underthrust the continental margin. Elevations are not unusually high, and grabens do not seem to be confined to regions of relatively high altitude. Thus, a convincing case cannot be made for the normal faulting being driven by gravity acting on an elevated region and its compensating crustal root. Instead, the extension has been ascribed either to a stress system caused by forces acting on the surrounding regions [9,10] or to drag on the bottom of the lithosphere [7], mechanisms that do not lend themselves to simple tests.

Whatever the cause of the extension in the northern Aegean area, a failure to explain it convincingly probably derives in part from inadequate

data describing where extension occurs, what orientations are common, what depths of faulting are involved, and how extension is related to other types of faulting. With this in mind we carried out an investigation of microearthquakes in northwestern Greece (Fig. 1), where fault plane solutions showed both normal and thrust faulting [12].

2. Region of study

Throughout most of the six weeks of recording from late July to early September 1979, we operated 18 instruments between the Ionian coast and the axis of the Pindos Mountains. The oldest rocks exposed in the area are Triassic evaporites, which are overlain by a few kilometers of limestones and dolomites [13]. Apparently no detrital material was deposited there during the Mesozoic. Finally in Eocene time the eastern part of the region began to receive detritus from the Pindos Mountains, which apparently had just risen above sea level. From Eocene time until the end of the Tertiary epoch carbonate and other detrital sediments accumulated in northwestern Greece. The total thickness of sedimentary rocks deposited on the Triassic evaporites reaches a few kilometers.

Significant tectonic activity in the region west of the Pindos apparently did not begin until the latest Oligocene or early Miocene [13]. This activity created folds and thrust faults that generally strike northwest-southeast and verge southwest, or more rarely, northeast. The location of this deformation seems to have spread westward from its beginning in Eocene time in the Pindos. Fault plane solutions from a few moderate earthquakes near the Ionian coast show thrust faulting and are consistent with slip on shallow-angle northeast-dipping planes [7,12]. Thus, these earthquakes reflect the same style of deformation implied for earlier periods by the structures now at the surface in regions farther inland. The southwestward vergence and migration of deformation as well as the fault plane solutions and studies of late Cenozoic deformation on Corfu, just west of the area in Fig. 1 [11] suggest that the tectonic activity results from collision and continuing northeastward convergence of the northern Ionian sea floor (which is

presumably underlain by continental crust) towards northwestern Greece.

While this convergence seems to continue, the active tectonics of northwestern Greece appears to be more complicated than the surface geology implies for earlier periods of the Tertiary era. Whereas the structures at the surface attest primarily to folding and thrust faulting, the active tectonics of northwestern Greece includes normal faulting. We are aware of no studies of Quaternary faulting or of surface breaks associated with major earthquakes in this portion of Greece, but the fault plane solution for one moderate event (1 May 1967) shows a large component of normal faulting [12]. However, some of our solutions for micro-earthquakes corroborate this style of deformation, and this more complicated tectonics is the subject of this paper.

Before discussing the seismic data let us note one other relevant aspect of the geology. Cross-sections drawn from the geologic map of northwestern Greece show that in many regions the Mesozoic and Cenozoic formations have become detached from the material below the Triassic evaporites [13]. The cross-sections are drawn with small amounts of underthrusting so that the package of Mesozoic and Cenozoic sediments is confined to the upper 5–7 km of the crust. Consequently nearly all of the earthquakes studied here would have occurred below the Triassic evaporites and therefore in a portion of the crust where the tectonic style might be very different from that at the surface. However, because the displacement on these thrust faults is very difficult to constrain, we probably should allow for the possibility that the Mesozoic sediments extend below 7 km depth.

3. Microearthquake investigation

During six weeks between July and September 1979, we operated a network of 18 portable seismographs in northwestern Greece (Fig. 1). The natural periods of the geophones were 1 second, and all recorded vertical components. Despite the lack of exposed crystalline basement rock and the need to install some stations on weak, weathered shales or fractured limestones, relatively high gains

were obtained (between 2.5×10^5 and 1.0×10^6 , corresponding to 78–90 db on Sprengnether MEQ-800 portable seismographs). Some 250 events with magnitudes between about 0 and 3 were recorded during a four-week period in which the whole array was fully installed and was functioning well.

The records were read using a lens and graticule with an estimated accuracy of 0.1 second for P-waves and 0.3 seconds for S-waves. Since these values are smaller than typical residuals that we subsequently calculated in the location process, we conclude that reading error is not significant in our procedure.

Among the 250 events that occurred between 9 August and 6 September, 167 were examined carefully because they were recorded by at least five stations with at least one clear S-phase at one of the closest stations. After initial tests with half space models, using the HYPO71 location program [14], these 167 events were located in 50 different two-layer structures using a starting depth of 5 km. These models had a depth for the interface that varied between 5 and 15 km and velocities ranging from 2.5 to 5.5 km/s in the first layer and from 5 to 6.5 km/s in the second layer. The structure finally selected had a surface layer 10 km thick with a P-wave velocity of 5.0 km/s overlying a half-space of 5.8 km/s. (For epicentral distances considered here, P- and S-waves refracted at the Moho would not be first arrivals so a Moho is not included.) This structure gave the lowest overall residuals among the 50 models considered. Changes of the depth of the interface of the model of ± 3 km and changes of the velocities by 10% from the chosen values did not alter epicentral locations for most events by more than 3 km and depths by more than 4 km. The v_p/v_s ratio used for both layers in the model was 1.78. Other values of v_p/v_s that retained low residuals also did not alter locations of most events more than 3 km horizontally or 4 km in depth. In general the error estimates determined by HYPO71 (ERH and ERZ) and by the foregoing tests were similar. From the 167 events, 19 were rejected either because their locations were found to depend strongly on the velocity structure or because HYPO71 gave values of ERZ greater than 8 km.

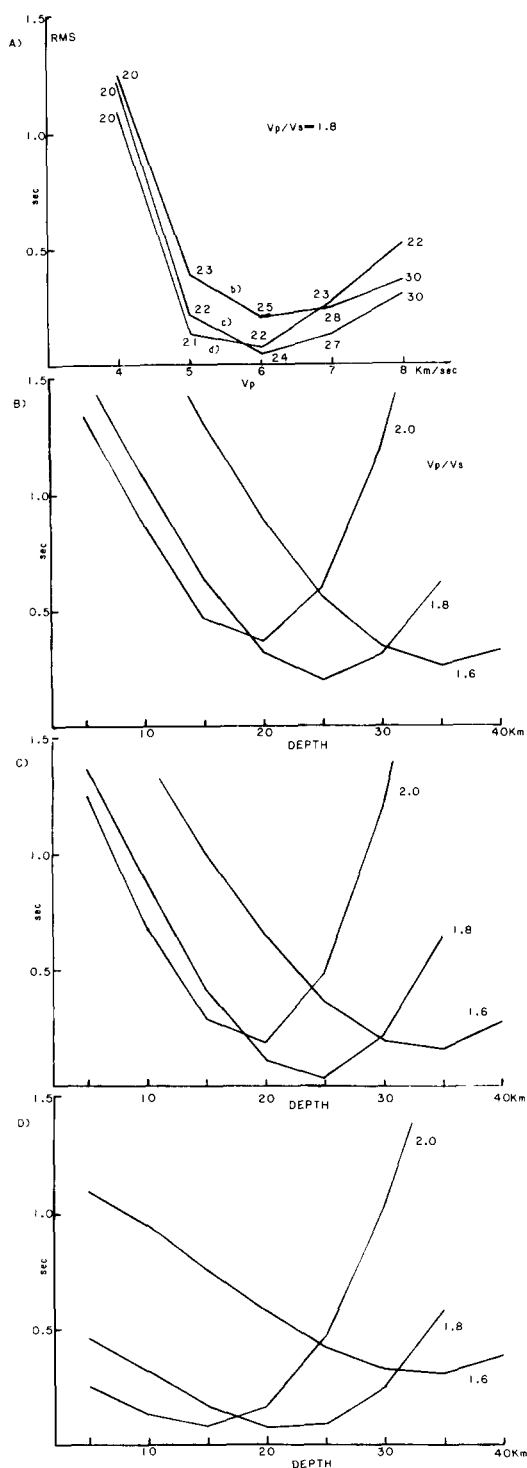


Fig. 2. Tests of the dependence of calculated depths on assumed velocity structures. A. The RMS residuals as a function

The RMS residuals for all the remaining events were less than 0.6 seconds, and most (94) were 0.3 seconds or less.

From the well located events we selected a reduced subset of 30 events, for which HYPO71 quoted ERH less than 2 km (solid circles in Fig. 1). All of these locations were based on more than 8 P-phases and more than 3 S-phases, and all had RMS residuals less than 0.3 seconds. On the basis of the tests that we performed, the locations of these events are thought to be uncertain by less than ± 2 km.

A surprising result of the study was that some events appeared to have depths of 20 km or greater. To demonstrate that these depths are reliable we show the results of some tests on three well recorded events near to the station VRO (Fig. 2, Table 1). We carried out the tests using half space models, which give slightly poorer locations than our layered model does. These tests, however, allow us to show in a simple way that even absurdly high or low P-wave velocities, or extreme v_p/v_s ratios do not shift the calculated depths very much. The events were first located with a wide range of half space velocities using a constant v_p/v_s ratio of 1.8. The P-wave velocities range from 3 to 8 km/s, well outside the range of either layer in our two-layer model. Even for extreme values of v_p and for locations with large RMS residuals (Fig. 2A), none of the calculated depths is less than 20 km. A half space velocity of 6.0 km/s was then adopted, and each event was located at various fixed depths using v_p/v_s ratios of 1.6, 1.8 and 2.0 (Fig. 2B, C, D). For the high ratio of 2.0 the minimum in residuals for one event occurs at 15 km, but in every other case the minimum occurs for depths greater than 20 km. A ratio of v_p/v_s 1.6 leads to greater inferred depths. We can therefore conclude that focal depths greater than 20 km are real.

of half space velocity for three events. A v_p/v_s ratio of 1.8 is used. The calculated depths of the events for each velocity is next to each point. The shallowest calculated depth is 20 km. In B, C, and D RMS residuals calculated from locating the events identified in A as b, c, and d in a half space ($v_p = 6$ km/s) with fixed depths are plotted as a function of those depths for v_p/v_s ratios of 1.6, 1.8 and 2.0. Note that minima are generally at 20 km or deeper.

TABLE 1

Events located at depths greater than 20 km. DMIN is the distance to the nearest recording station, and GAP is the largest azimuthal gap between stations. Columns P and S give the number of P and S arrivals, respectively, used in computing the location. The letters b, c, and d correspond to those used in Fig. 2A

| Event | Date | Origin time | Latitude (°N) | Longitude (°E) | Depth (km) | DMIN (km) | GAP (°) | P | S |
|-------|---------|---------------|---------------|----------------|------------|-----------|---------|----|---|
| b | 1/8/79 | 12: 48: 44.17 | 39.713 | 20.515 | 25.1 | 7.6 | 137 | 12 | 7 |
| c | 2/8/79 | 13: 13: 48.03 | 39.710 | 20.534 | 24.1 | 7.3 | 131 | 8 | 5 |
| d | 11/8/79 | 20: 09: 12.17 | 39.716 | 20.507 | 21.9 | 8.0 | 193 | 13 | 8 |

4. Distribution of earthquakes

The map of epicenters (Fig. 1) shows that earthquake activity is diffusively distributed over a broad area. There are relatively large areas without activity, and there is a clustering of activity in two relatively small regions. The recording period was too short to allow reliable inferences about where activity is likely to be high or low over a long period of time. Nevertheless, the data clearly show that the earthquakes do not all occur on a single

fault, or a small number of major faults.

Many foci are surprisingly deep. Although no events were located at intermediate depths, one well located event occurred at a depth of about 29 km (shown in Fig. 1) and a histogram of the depths of the 30 most reliably located events reveals a clustering near a depth of 18 km (Fig. 3A). A similar histogram (Fig. 3B) for all 148 events located here reveals the same peak at 18 km, and a second larger one near 10 km. The depth constraints on events used to produce the second histogram are poor and the peak of activity near 10 km may be a consequence of the interface at that depth. However, we have excluded 15 events with calculated depths actually at 10 km from this histogram. The most convincing reason for supposing the maximum at 10 km to be real is that it appears on the histogram of the best located events (Fig. 3A). There are few well located events at depths of 10 km because, with the density of stations in this array, the epicentral distance to the nearest recording station often is greater than such shallow focal depths. Whatever the distribution of these shallow events, the minimum in activity near 15 km appears to be real.

The depth distribution suggests that most of the seismicity occurs below the Triassic evaporites. Even if one allows for an error of a factor of two in the inferred 7 km depth of this horizon [13], most earthquakes occur below it. Only if there has been considerably more crustal shortening than the Greek and French geologists inferred, so that the Mesozoic and Cenozoic sediments overthrust one another to form a greatly thickened stack, could the earthquakes occur within these formations. More likely, the microearthquakes occurred below the Triassic evaporites in Paleozoic sedi-

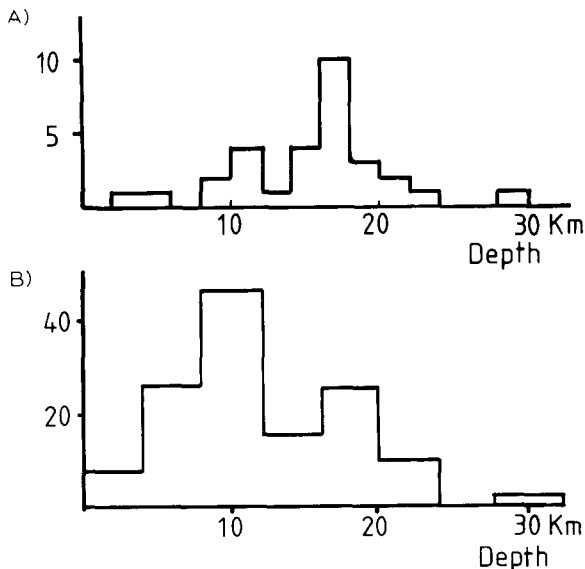


Fig. 3. Histograms of calculated depths for the 30 best located events (A) and for all 148 events (B). Note that criteria for well constrained depths tend to eliminate the shallower events and therefore to bias the histogram for the well located events (A) towards greater depths than when such criteria are relaxed. Nevertheless the minimum of depths at about 15 km can be seen in both histograms.

ments or crystalline basement. If the younger formations are detached at the Triassic evaporite horizon, we might expect them to reveal a different tectonic style from the material beneath them.

5. Fault plane solutions

We determined eight reliable fault plane solutions for microearthquakes (Fig. 4, Table 2) using only rays thought to be radiated into the upper focal sphere. (For the purposes of presentation, however, first motions are plotted on the lower hemisphere.) These eight solutions, plus two solutions for larger events based on teleseismically recorded phases [12,15] are plotted in Fig. 1. Soufleris [16] showed that epicenters of earthquakes in Greece determined by the U.S. Geological Survey are often as much as 20 km north of the zones of maximum intensity. Consequently, we plotted the epicenters of these two events in the

centers of the regions that suffered the most damage.

The fault plane solutions vary widely: Several solutions (9, 17, 18, 19, 20 and 69.10.13) show thrust or reverse faulting and in most cases can be interpreted as reflecting north-south to northeast-southwest crustal shortening. At the same time several others (15, 23, 26 and 67.5.1) show normal faulting and seem to indicate extension in the perpendicular direction. This pattern, however, is not without exceptions. The P axis for 19 trends NNW-SSE instead of north-south or northeast-southwest like those for 9, 17, 18, 20 or 69.10.13. The solutions for 15 and 26 indicate normal faulting but with extension approximately north-south and northwest-southeast, respectively, and therefore parallel to the directions of shortening implied by some of the other solutions. It is possible that 19, which occurred near to the edge of the array, could have a solution more consistent with northeast-southwest shortening if points near to

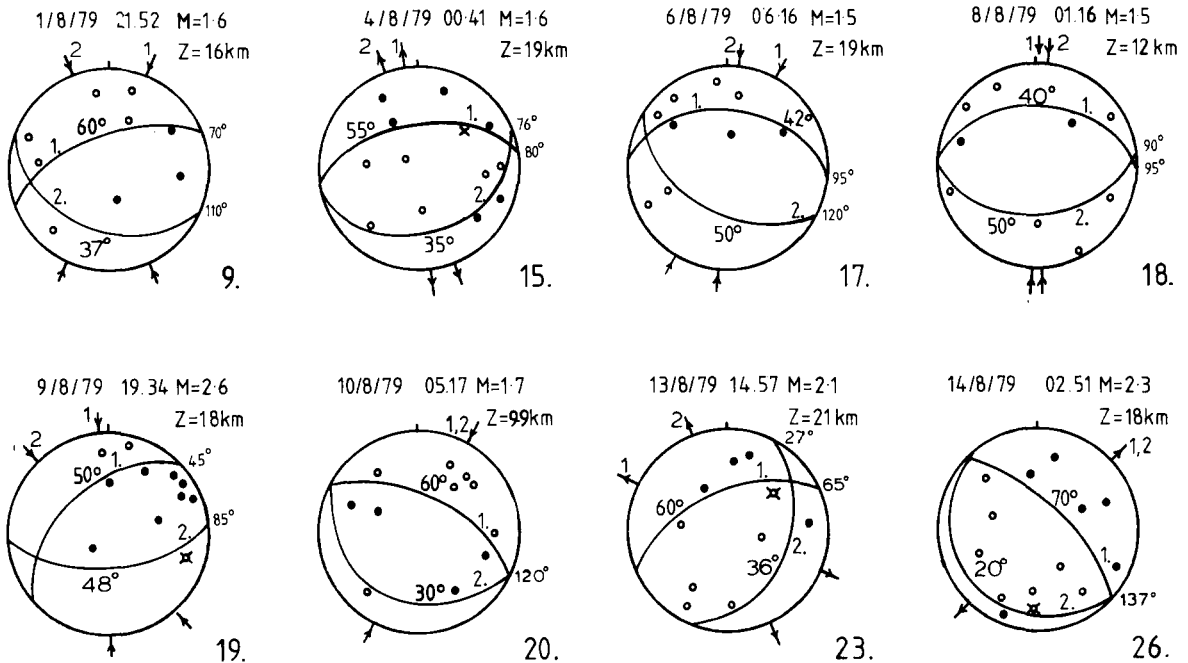


Fig. 4. Lower hemisphere projections of focal spheres showing the distribution of polarities. Solid circles represent compressional P-wave first motions and open circles dilatations. Circles with crosses through them denote small arrivals. Arrows at the edges of the diagrams show the horizontal components of possible slip vectors. The numbers (1 or 2) index the plane to which they refer. We assume that all rays were radiated into the upper hemisphere, but we plot them on the lower hemisphere assuming point symmetry of the radiation pattern.

TABLE 2

Fault plane solution parameters

| No. | Plane 1 | | Plane 2 | | P axis | | T axis | | B axis | |
|-----|------------|---------|------------|---------|-----------|------------|-----------|------------|-----------|------------|
| | Strike (°) | dip (°) | strike (°) | dip (°) | trend (°) | plunge (°) | trend (°) | plunge (°) | trend (°) | plunge (°) |
| 9 | 70 | 60 | 110 | 37 | 356 | 12 | 116 | 67 | 262 | 20 |
| 15 | 80 | 55 | 76 | 35 | 180 | 80 | 348 | 10 | 79 | 2 |
| 17 | 95 | 42 | 120 | 50 | 198 | 5 | 89 | 77 | 289 | 13 |
| 18 | 95 | 40 | 90 | 50 | 182 | 5 | 336 | 84 | 92 | 3 |
| 19 | 45 | 50 | 85 | 48 | 335 | 1 | 68 | 69 | 244 | 21 |
| 20 | 120 | 60 | 120 | 30 | 30 | 15 | 210 | 75 | 120 | 0 |
| 23 | 65 | 60 | 27 | 36 | 197 | 68 | 320 | 13 | 54 | 18 |
| 26 | 137 | 70 | 137 | 20 | 227 | 65 | 47 | 25 | 137 | 0 |

the edge of the focal sphere were interpreted as refracted rather than direct arrivals. By similar reasoning, the solution for 26 could possibly be changed from normal faulting to reverse or thrust faulting on a very steeply or a very gently dipping plane. Nevertheless, although it is possible that the fault plane solutions most different from one of the two typical types are, in fact, incorrect, there remains a wide range of solutions.

Although the events with normal faulting are among the deepest and occur only in the southeastern part of the region studied, it is probably unwise to conclude that this pattern in depth applies to the whole area or that the regional distribution of normal and thrust faulting applies for longer periods of time. At the same time, the variations in the orientations of the nodal planes, even if grouped by fault type, require variations in the sense of slip and in the style of deformation throughout the region. Deformation is clearly not homogeneous on scales of tens of kilometers. This inhomogeneous deformation is almost certainly the result of heterogeneities in strength and in stress, heterogeneities that could result from pre-existing fractures or from contrasts in mechanical properties such as those arising from the juxtaposition of different lithologies (Fig. 5).

6. Summary and geologic interpretation

The seismicity and fault plane solutions of microearthquakes in northwestern Greece reveal

complicated deformation. Earthquake activity is widely distributed and cannot be attributed to slip on a small number of well defined faults. Depths of foci are mostly between 10 and 25 km, with maxima in activity near 10 and 18 km. Thus most of the activity is probably below the Mesozoic and Cenozoic sedimentary rocks that cover the region and that are detached from the underlying older sedimentary rocks and basement on a Triassic

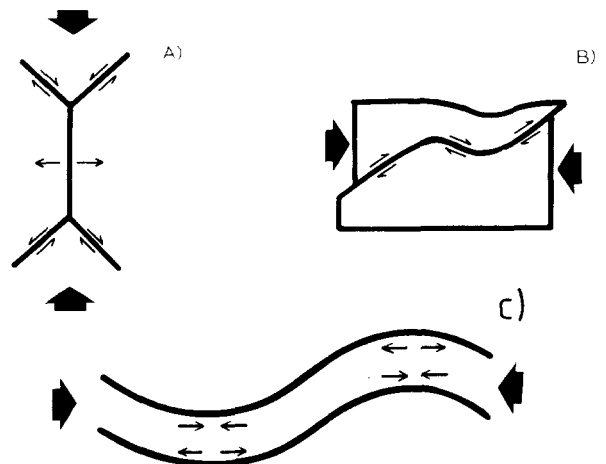


Fig. 5. Mechanisms that can markedly perturb the local stress field and therefore cause earthquakes with fault plane solutions different from those reflecting overall crustal shortening. A. Strike slip faulting and extension normal to the direction of maximum compressive stress. B. Normal faulting produced by a variation in the dip of an otherwise thrust fault. C. Extension and compression associated with the bending of a strong layer embedded in weaker and more easily deformed surrounding formations.

evaporite sequence. The ten fault plane solutions differ from one another and reveal both thrust faulting (in most cases caused by northeast-southwest to north-south crustal shortening), and normal faulting, (usually reflecting northwest-southeast extension). This deformation may form part of a regional strain field that includes both northeast-southwest shortening and northwest-southeast extension, but that is also perturbed by stress concentrations associated with heterogeneous mechanical behavior.

The complicated tectonics of northwestern Greece clearly are not easily ascribed to variations in altitude and compensating crustal thickness, for there is no correlation between the type of faulting and the elevations in the epicentral region (see typical cross-section in Fig. 1). Nor are the variations in fault plane solutions easily ascribed to drag on the bottom of the lithosphere as McKenzie [7] suggested. First, the orientation of slip vectors of the normal faults and thrust faults are not in general parallel as McKenzie assumed, and second, there are not two parallel zones of normal and thrust faulting. Moreover, the short distance between earthquakes with very different types of faulting cannot be due to stress applied to the bottom of the plate some 10's to 100 km below the depths of the earthquakes.

Compression applied to the edges of the region can account for a regional crustal shortening and crustal extension in a perpendicular direction. The northwestward convergence of the Adriatic and Ionian sea floors towards the Aegean sea floor probably causes the crustal shortening in that direction. Nevertheless, although forces applied to the boundaries can account for at least part of the average crude regional stress field, the local variations in fault plane solutions are probably due to slip on pre-existing zones of weakness or local perturbations in the stress field associated with contrasts in lithology. The thrust faulting would then be a direct manifestation of crustal shortening and continental convergence. Some of the normal faulting might be due to extension perpendicular to the direction of shortening and could reflect a wedging apart of blocks along weak zones oriented favorably for such a process (Fig. 5A). The solution for event 26, which indicates normal

faulting with extension parallel to the apparent direction of regional compression could result from uneven slopes on gently dipping or horizontal thrust planes (Fig. 5A) or might result from stress concentrations associated with the formation of folds in relatively competent beds surrounded by weaker strata (Fig. 5B). In any case, regardless of whether or not any of the specific mechanisms shown in Fig. 5 for perturbing the local stress field applies to the fault plane solutions shown here, we think that it is very likely that the variation in fault plane solutions is due to local heterogeneities in the stress field and not necessarily to large-scale regional variations in it.

Acknowledgements

We thank B. Papazachos and P. Voidomatis for field and logistic support, Diana and Peter King and Peter Sherwood for helping operate the instruments, M. Barazangi and D. Hatzfeld for critically reviewing the manuscript, and D. Frank for typing it. The project was supported by the National Environment Research Council GR3/3904 and the H.O. Wood fund of the Carnegie Institution of Washington, D.C. This is Cambridge Earth Sciences Contribution Number ES389.

References

- 1 P. Molnar and P. Tapponnier, Cenozoic tectonics of Asia: effects of a continental collision, *Science* 189, 419–426, 1975.
- 2 P. Tapponnier and P. Molnar, Active faulting and Cenozoic tectonics of the Tien Shan and Mongolia and Baykal regions, *J. Geophys. Res.* 84, 3425–3459, 1979.
- 3 P. Molnar and P. Tapponnier, Active tectonics of Tibet, *J. Geophys. Res.* 83, 5361–5374, 1978.
- 4 B. Dalmayrac and P. Molnar, Parallel thrust and normal faulting in Peru and constraints on the state of stress, *Earth Planet. Sci. Lett.* 55, 473–481, 1981.
- 5 L. Royden, Evolution of the Pannonian Basin System and its relationship to the Carpathian Mountain system, 256 pp., Ph.D. Thesis, M.I.T., 1981.
- 6 X. Le Pichon and J. Angelier, The Hellenic Arc and trench system: a key to the Neotectonic evolution of the Eastern Mediterranean area, *Tectonophysics* 60, 1–42, 1979.
- 7 D. McKenzie, Active tectonics of the Alpine-Himalayan belt: the Aegean Sea and surrounding regions, *Geophys. J. R. Astron. Soc.* 55, 217–254, 1978.

- 8 J.A. Jackson, J. Gagnepain, G. Houseman, G.C.P. King, P. Papadimitriou, C. Soufleris and J. Virieux, Seismicity, normal faulting, and the geomorphological development of the Gulf of Corinth (Greece): the Corinth earthquakes of February and March 1981, *Earth Planet. Sci. Lett.* 57, 377–397, 1982.
- 9 J.F. Dewey and A.M. Celal Sengör, Aegean and surrounding regions: complex multiplate and continuum tectonics in a convergent zone, *Geol. Soc. Am. Bull.*, Pt. 1, 90, 84–92, 1979.
- 10 P. Tapponnier, Evolution tectonique du système alpin en Méditerranée: poinçonnement et écrasement rigide-plastique, *Bull. Soc. Géol., Fr.* (7), XIX/3, 437–460, 1977.
- 11 J.L. Mercier, N. Delibassis, A. Gauthier, J.J. Jarrige, F. Lamille, H. Philip, M. Sebrier and D. Sorel, La néotectonique de l'Arc Egéen, *Rev. Géol. Dyn. Géogr. Phys.* 21, 67–92, 1979.
- 12 D.P. McKenzie, Active tectonics of the Mediterranean region, *Geophys. J. R. Astron. Soc.* 30, 109–185, 1972.
- 13 L'Institut de Géologie et Recherches du sous-sol-Athènes et l'Institut Français du Pétrole-mission Grèce, *Etude Géologique de l'Epine (Grèce Nord-Occidentale)*, 306 pp., 1966.
- 14 W.H.K. Lee and J.C. Lahr, HYPO71 (revised): a computer program for determining hypocenter, magnitude, and first motion pattern for local earthquakes, U.S. Geol. Surv. Open-file Rep. 75-311, 113 pp., 1975.
- 15 J.A. Jackson, personal communication, 1983.
- 16 C. Soufleris, The 1978 earthquake sequence near Thessaloniki (northern Greece), Ph.D. Thesis, Cambridge University, Cambridge, 1981.